RSC Advances

PAPER

View Article Online
View Journal | View Issue

Elastic properties of natural single nanofibres†

Cite this: *RSC Adv.*, 2014, **4**, 11225

F. M. Fernandes,‡*[a] L. Vázquez,[a] E. Ruiz-Hitzky,[a] A. Carnicero[b] and M. Castro[c]

Received 9th December 2013
Accepted 10th February 2014

DOI: 10.1039/c3ra47452f

www.rsc.org/advances

Natural nanomaterials are becoming increasingly relevant in the context of mechanical reinforcement of a multiplicity of matrices. The elastic properties of single nanomaterials are, however, mostly unknown. By combining two different – and complementary – AFM strategies we determined the elastic properties of single clay sepiolite nanofibres to be 8.2 ± 2.5 GPa in bending mode. We took advantage of the silanol-rich sepiolite surface to covalently graft it onto a micropatterned silicon substrate to achieve an experimental setup with clearly defined boundary conditions. The determination of the elastic properties of single nanofibres was completed by the determination of the elastic moduli at other length scales and their behaviour from the macro- to the nano-scale is discussed.

Introduction

Naturally occurring nanomaterials are attracting increasing attention in the field of nanoscience due to their outstanding performance and widespread availability. Moreover, this type of nanoparticles is especially appealing since their production does not require complex or costly synthetic procedures. Natural nanoparticles can be divided into two main groups according to their origin: biological or geological. Nanoparticles from biological origin are usually found in nature integrated in rather complex hierarchical systems. In general, such systems present a strict organization of their components: hydroxyapatite nanocrystals in bone, cellulose in wood[1] or aragonite in nacre,[2] are few examples of systems where the meticulous distribution of the reinforcing elements in nanocomposites allows to maximize their performance. In contrast, geological nanoparticles are significantly less organized in their occurring media. Using geo-nanoparticles in the preparation of nanocomposites presents, therefore, a potential advantage in comparison with those obtained from biological entities. Their relatively low degree of organization allows to obtain nanobuilding blocks for the production of new natural nanoparticle-based constructs without the need to disassemble systems whose properties are already maximized. Among the most scientific and technologically relevant geo-nanoparticles are clay minerals. Since the seminal work by Fukushima's group in the context of polymer–clay nanocomposites (PCN),[3,4] these materials have attained a leading role in materials science. In particular, sepiolite – a hydrated magnesium silicate displaying a fibrous habit[5] with a diameter varying between 50 and 100 nm and a length in the micron range – has recently found widespread application in both functional and structural materials. Its nano-dimensions and unusual textural features (Fig. 1) along with an easily addressable surface chemistry have drawn sepiolite to the spotlight of functional materials with properties "a la carte". To cite a few examples, it has been used in bionanocomposite formulations for influenza virus carrier in vaccines[6] or as a supporting phase in the development of graphene-like materials from natural resources.[7–9]

In the context of polymer–clay nanocomposites firstly introduced by Fukushima's group, sepiolite is less known than its layered counterparts such as mica and montmorillonite.

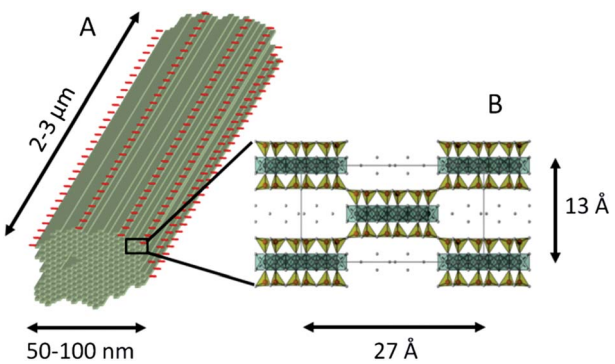

Fig. 1 (A) Microstructure of a sepiolite natural nanofibre; and (B) sepiolite crystalline structure showing Si tetrahedra (in yellow) and Mg octahedral (in green), viewed along the *c* axis according to Brunauer and Preisinger.[5] Oxygen atoms (in grey) representing water molecules are visible within the channels and tunnels of the fibres.

[a]*Instituto de Ciencia de Materiales de Madrid, CSIC, C/Sor Juana Inés de la Cruz, 3, 28049 Madrid, Spain*

[b]*Departamento de Ingeniería Mecánica and DNL, Universidad Pontificia Comillas, Madrid, Spain*

[c]*GISC and Grupo de Dinámica No Lineal, Universidad Pontificia Comillas, Madrid, Spain*

† Electronic supplementary information (ESI) available: Elastic measurements conditions summary and a succinct description of the mechanical model used. See DOI: 10.1039/c3ra47452f

‡ F.M.F is presently at the Laboratoire de Chimie de la Matière Condensée de Paris, UPMC Univ. Paris 06, UMR7574, Collège de France. 11 Place Marcelin Berthelot, 75231 Paris cedex 05, France. E-mail: francisco.fernandes@upmc.fr

Nevertheless, this magnesium silicate has recently found increasing relevance in the reinforcement of biopolymer matrices. The most notable example refers to its incorporation in polysaccharides such as chitosan[10,11] and starch[12] or in the reinforcement of polypeptides such as collagen[13] and gelatine[14–16] where applications in tissue engineering are envisaged. To a lesser extent, it has been applied in the reinforcement of epoxy and polyurethane matrices[17].

Following what has become a common scenario, the chemical and functional properties of nanomaterials such as single clay nanoparticles have been thoroughly described long before the determination of their mechanical properties[18–21]. This feature is no doubt linked to the technical difficulties in directly probing the mechanical properties of nanoparticles. Some theoretical work regarding the mechanical properties of layered silicates is available but reported results scatter significantly over some orders of magnitude.[22,23] Also, assessment of the mechanical properties of layered clay stacks has been experimentally addressed[24,25] but no work is available on single crystalline entities such as a clay lamellae or a single clay fibre. In general, both layered and fibrous clays are extensively used in the reinforcement of polymeric matrices but the key element to rationally design structural nanocomposites, the filler mechanical properties, is still missing. In addition, the inference of sepiolite nanofibres mechanical properties from the measurements performed on the resulting nanocomposites is delicate and error prone. It has been recently shown that for sepiolite-based bionanocomposites[15,16] – where the orientation of the reinforcing nanofibres was known, and thus the adequate model could be chosen to describe the composite's elastic properties – the presence of sepiolite tends to dramatically influence the crystallinity of polymeric matrices. It becomes then impossible to obtain coherent values for the elastic properties of the nanofibres since the values of the matrix itself vary according to the clay loading. However, the same features that are likely to induce the crystallization of polymeric materials, structural silanols on the edges of sepiolite fibres, become the key elements for the reproducible *in situ* quantification of sepiolite elastic properties by means of Atomic Force Microscopy (AFM) as showed below.

Experimental section

Functionalization of sepiolite fibres

Sepiolite-(3-aminopropyl)trimethoxysilane derivative (SEP-APS) was used for mechanical testing due to two key factors. Firstly, the presence of the amino functions on its surface is advantageous because it allows covalently grafting sepiolite nanofibres to the functionalized silicon substrate. This strong grafting procedure hampers the displacement of sepiolite fibres while scanning the surface with the AFM probe. The second factor is the nature of SEP-APS modification itself. Because sepiolite presents silanol groups only in the external blocks of its structure, its internal structure is not affected by the organosilane grafting, which occurs solely on the mineral edges. Specifically, sepiolite fibres were functionalized by grafting APS to the mineral surface. Sepiolite (3% w/v) was dispersed in 200 ml of isopropanol in a two neck round bottom flask equipped with a reflux column. After vigorous agitation the temperature was set to 65 °C and 25 ml of the organosilane were added. The reaction was left to proceed overnight. After cooling the mixture down to room temperature, it was filtered and thoroughly washed with water–methanol (1 : 1) mixture. The resulting solids were dried at 60 °C under dynamic vacuum for 24 hours and stored in plastic vessels. The resulting organo-modified sepiolites were characterized by CHN chemical analysis and FTIR.

Preparation of an adequate rigid patterned substrate

In principle, crystalline silicon surfaces are adequate substrates for nanomechanical testing of suspended nanofibres due to its high rigidity as well as to the technological availability to nanopattern it.[26] Moreover, its surface can be easily modified with organosilanes after an oxidative step with acid "piranha" solution.[27] Thus, crystalline silicon nanopatterned with 500 nm deep and 1.5 μm in diameter wells (from IMB-CNM, Barcelona, Spain) was used. The chemical pre-treatment was designed to ensure covalent bonds between the SEP-APS and the silicon substrate. To achieve a reactive, silanol-rich layer on silicon wafers, these were treated with "piranha" solution (7 : 3 volume ratio mixture of 30% H_2O_2 and concentrated H_2SO_4) for one hour at ambient temperature. After thorough rinsing with bi-distilled water, wafers were dried overnight at 60 °C. Wafers were subsequently immersed in a solution of (3-glycidyloxypropyl)trimethoxysilane (GOPS) in toluene (0.5%) for four hours at 60 °C. Afterwards silicon wafers were rinsed with toluene and dried under dynamic vacuum at the same temperature.

Dispersion of sepiolite fibres over the patterned substrate and covalent grafting

The deposition of SEP-APS nanofibres in the GOPS-modified wafer was prepared by dispersing 10 ppm SEP-APS in toluene, depositing one drop over the nanopatterned modified wafer and allowing it to dry at ambient temperature. Wafers were then placed in an oven at 60 °C to promote covalent grafting of the APS and GOPS fraction of each substrate (fibre and wafer respectively).

Identification of isolated fibres suspended over specific wells by FE-SEM

Field Emission-Scanning Electron Microscopy (FE-SEM) allowed determining which fibres were individually deposited over the wells. Sepiolite-modified silicon wafers were observed in a FEI Microscope, Nova NanoSEM 230 model without previous sputtering process to ensure that sepiolite's mechanical properties would not be affected by the deposition of metallic layers. Samples were imaged at 2500× magnification throughout the entire nanopatterned area of interest. Beam landing energy (2 keV) and spot size were set to minimize damaging sepiolite fibres, ensuring at the same time reproducibility throughout the different imaging sessions. FE-SEM images were juxtaposed to permit conclusive pin-pointing of nanofibres in conditions to be measured under the AFM.

Mechanical testing using the Atomic Force Microscope (AFM)

The first step is localizing the previous identified hanging fibres to be analyzed by AFM. For that purpose, we have employed a Nanoscope IIIa equipment coupled to an optical microscope. The latter helps us to address the tip to the area where the fibre was localized by FE-SEM. Once the tip is engaged in this region, a large area ($50 \times 50\ \mu m^2$) is scanned in contact mode in order to find the specific fibre. Once the fibre is located, the scan size is reduced down to $3 \times 3\ \mu m^2$, in order to perform the nanomechanical testing. In these measurements, the tip load is kept at minimum in order to not damage the fibre and/or the tip itself.

In these studies we employed silicon cantilevers (DLever, Veeco, USA) whose spring constant (in the 0.5–2 N m^{-1} range) was measured by the thermal tuning method. The sensitivity of the cantilever was also calibrated on a hard fused silica surface.

The mechanical study of the sepiolite fibre was done using the two methods detailed below and the model for the bending of a clamped elastic beam disclosed in the ESI section.† The sepiolite nanofibres diameters were systematically determined by measuring the height of each fibre throughout their fully supported ends. The obtained values were averaged to obtain a representative value corresponding to each fibre diameter.

Sequential imaging at different force loads

This method consists of imaging the same narrow area containing the chosen fibre under the same operational conditions but at different increasing force loads. At the end of the experiment, we performed one last measurement at the initial low force in order to ensure that the fibre was not altered by the measurement. The fibre profile obtained in each condition was analysed and the deflection of the fibre was derived for each applied force. From these data, provided that the dimensions of the nanofibre are known, it is possible to obtain a plot of the applied stress on the nanofibre *versus* the strain or fibre deformation. In the ideal case where the force is applied exactly in the middle of the suspended length of the nanofibre and this presents a uniform radius and a circular cross-section the resulting slope of such plot is the elastic modulus of sepiolite in bending mode.

Force volume

This mode consists in the sequential collection of different force measurements over a given area.[28] In this case, the area corresponds to a narrow one where a hanging nanofibre has already been spotted. The procedure includes the determination of this area of interest and dividing it into a predefined grid. In this work the area was divided into a 64×64 grid, whose force profiles were collected. At the end of the experiment a standard contact mode image was taken in order to check that the nanofibre was not damaged or altered by the measurements. This technique quantitatively characterizes the mechanical properties of each point in the image. By selecting the points where the nanofibre is hanging over the well, it is possible to directly obtain a force *versus* fibre deformation information. Specifically, the cantilever deflections were measured on the microfibrils in the middle position of the span and the substrates to obtain the force curves. The deformation of the substrate occurring during force curve measurement could be eliminated, because the Si wafer was sufficiently stiff for its deformation to be negligible. The procedure to derive the fibre deflection from the force curves is the standard one, already used on other microfibril systems.[29] Since the fibre was bent by the tip load, the deflection of the cantilever on the fibre was attributed to the difference between the *z*-piezo displacement and the deflection of the fibre. Hence, the deflection of the sepiolite fibre was determined by subtracting the deflection of the cantilever on the fibre from that on the substrate. Finally, the applied force was obtained as the product of the cantilever deflection and its spring constant. It is worth noting that this method samples the mechanical response of the nanofibre in a very shorter time than the sequential imaging method and with a much higher sampling data.

Nanoindentation of sepiolite blocks

These experiments were performed with a Nanoindenter Nanotest from Micro Materials Ltd., operating with a Berkovich indenter. The blocks were previously machined into approximately $5 \times 5 \times 5\ mm^3$ cubes and its surface successively polished with SiC paper into a smooth, scratch-free surface under naked eye inspection. The sample surface was evaluated by means of 20 indentations per maximum load selected, namely 0.3, 1, 3, 5 and 25 mN. In order to obtain the elastic modulus of the sample, we have applied the Oliver–Pharr model.[30] In this analysis, we have used as the Young's modulus and Poisson rate of the indenter the known values of 1141 GPa and 0.07, respectively. As the Poisson rate of the sepiolite is not known, and most materials present values ranging between 0 and 0.5,[31] we have taken into account both values to calculate the limit values for the sepiolite's elastic modulus.

Mechanical properties of macroscopic blocks of sepiolite: sepiolite blocks were machined to approximately $10 \times 10 \times 10\ mm^3$ pieces for compression testing. The cutting process proceeded in such manner that it was possible to maintain information about the orientation of each single sepiolite monoliths with respect to the main block. Such information is relevant as it allows discriminating the mechanical properties according to the direction of the compression experiment. The obtained results from several experiments in the three different directions indicate the absence of clear detectable macroscopic anisotropy of the mechanical properties. The mechanical characterization of the prepared materials was performed in an Instron 3345 Universal Testing Machine equipped with 500 N load cell.

Results

The strategy reported in the present work takes advantage of the presence of easily available silanol groups in the surface of sepiolite to promote a covalent bond between the single sepiolite fibres and a patterned silicon substrate (Fig. 2). Such bond permits to perform traditional beam bending experiment but at the nanoscale with clearly defined boundary conditions: the

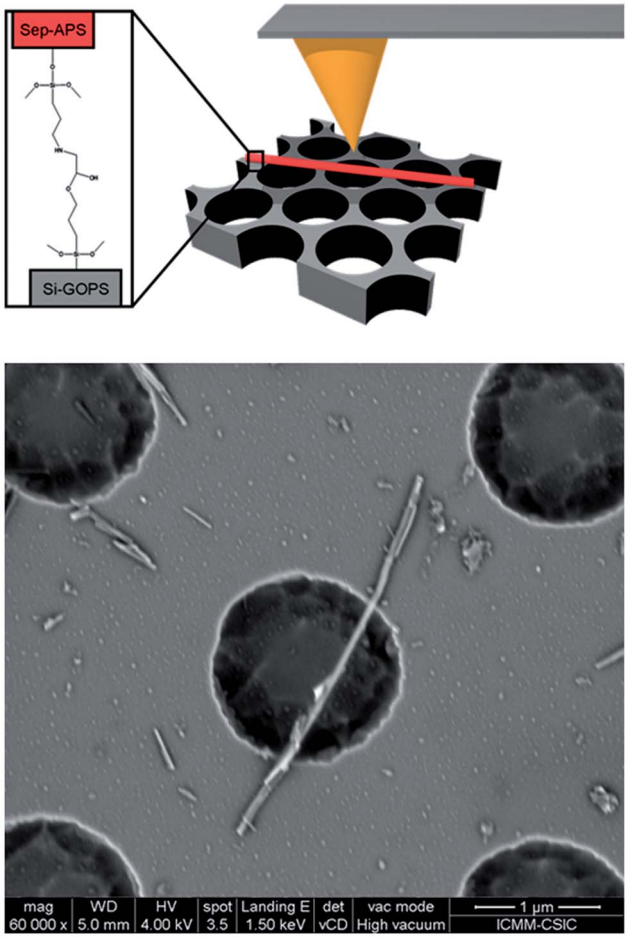

Fig. 2 On the top left, illustration of the covalent grafting between a sepiolite nanofibre and the micropatterned silicon wafer. On the top right, AFM experimental setup displaying the suspended nanofibre over a microwell as well as the AFM tip. Bottom, FE-SEM image of a suspended sepiolite nanofibre hanging over a 1.5 μm well.

clamped–clamped beam. Conceptually, the characterization of the mechanical properties of a nanofibre is simple. It consists in the deposition of a nanofibre with known dimensions over a known suspended length and measuring the required force to induce a given deformation or *vice versa*, as previously demonstrated for carbon nanotubes.[32,33]

Nevertheless, the experimental requirements to achieve such simple picture using an AFM are far more complex than the concept itself. It involves the following steps: (1) functionalization of sepiolite fibres, (2) preparation of an adequate rigid patterned substrate, (3) dispersion of sepiolite fibres over the patterned substrate accompanied by the respective covalent grafting, (4) Field Emission-Scanning Electron Microscopy (FE-SEM) detection of isolated fibres suspended over specific motifs in the patterned substrate, and (5) mechanical testing using the Atomic Force Microscope (AFM). We achieved the previously mentioned first and second steps through sol–gel chemistry reactions, notably the condensation of organo-alkoxysilanes onto the silanol groups present on sepiolite surface and on the silicon micropatterned substrate. Sepiolite was modified with (3-aminopropyl)trimethoxysilane while (3-glycidyloxypropyl) trimethoxysilane was utilized to modify the silicon micropatterned substrate after brief activation by means of piranha solution. The presence of the amino moiety on the surface of sepiolite is then covalently grafted to the epoxy functions in the silicon wafer (Fig. 2). After steps (3) and (4) have been accomplished, and the nanofibres under study are located, the AFM cantilever is used as a mechanical probe working in different modes: contact, force curve and force volume. The mechanical properties of the nanofibre are obtained by correlating the applied force to the induced fibre deflection.

Assaying the mechanical properties of the sepiolite nanofibres was accomplished using two different AFM setups namely, sequential imaging in contact mode at different applied loads and force volume. The advantage arising from such dual determination lays on the complementarity between these two approaches. Thus, in the sequential imaging method, in which the fibre is aligned along the *x*-axis of the AFM images, the fibre is continuously under the tip load although at different locations. In contrast, in FV the tip load is applied and relaxed in less than 0.5 s on a given point of the fibre, which has already recovered of the previous load event. Therefore, the comparison of the results obtained by these two approaches allows to cross-validate them.

In Fig. 3 we show the results obtained by this technique for different samples. Although the AFM measures force (nN) and deflection (nm), we summarize the information in the standard form: stress (GPa) *vs.* strain (non-dimensional). To extract the information about the elastic properties of the nanofibre, we use the classical theory of Euler–Bernoulli[34] of the bending of an elastic beam encastré in both ends and subjected to an external force (see ESI for details†). Within this theory, it is mandatory to determine whether the beam (in our case, the nanofibre) is clamped at its ends or simply supported. The major factor accounting for the choice of the clamped–clamped beam model relates to the fact that the beam (sepiolite fibre) is functionalized with an amino-terminated organosilane while the supporting structure (silicon chip) is modified with an epoxy terminated moiety. These two functional groups react in a

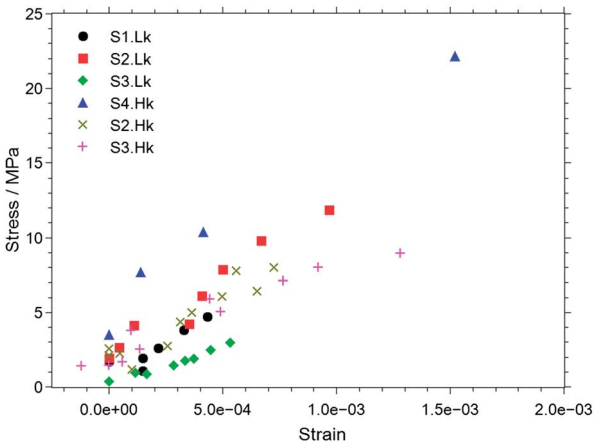

Fig. 3 Stress–strain plot obtained from deflection results measured under the AFM of four samples (S1 to S4) measured using two different AFM probes. Cantilever elastic constants are Lk = 0.76 N m^{-1} and Hk = 1.74 N m^{-1}.

straightforward manner to generate a strong covalent bond, which promotes a strong adhesion between the fibre and the substrate. As a consequence, the fibre is irreversibly bound to the substrate as depicted in the reversible deformation observed in Fig. 4. When the beam deflection is measured at the same point where the force is applied, we can assume that the deflection δ of a nanofibre of suspended length L, when subjected to a force, F, applied at a distance x from the closest end, is given by,

$$\delta = \frac{Fx^3(L-x)^3}{3EI_0L^3}, \quad (1)$$

where E is the elastic bending modulus and I_0 is the area moment of inertia of the nanofibre cross-section (considered to be a circle).

The values so obtained for the elastic modulus do not differ considerably; being the average value for the elastic modulus of sepiolite fibre (determined with the current approach) around 8.2 GPa with a standard deviation (sd) of 2.5 GPa. Although the sd is large when compared to the absolute value of sepiolite's modulus (*circa* 30%), it is important to take into consideration some aspects regarding the application of non-standard methods for mechanical characterization of nanomaterials. The first relates to the intrinsic variability of the mechanical properties of sepiolite that, along with the anisotropy associated with the crystalline structure of sepiolite might account for the attained standard deviation. On the other hand, the reported strategy is time consuming, which leads to a limited amount of data points per sample. In addition, an estimation of the errors involved in the measurements, whose principal source is the error associated with the AFM data, close to 5%, implies errors in the measured fibre diameter and length as well as in the determination of the middle point of the fibre that finally results in an error bar in E of one third. As previously mentioned, an alternative way to obtain force information is by means of the "force volume" mode of the AFM.[28]

The value of this approach is threefold: firstly, it allows to independently validate the information obtained by the previous procedure (and thus validate the methodology itself), secondly, it permits to explore the consistency of both approaches and finally it supplies a substantive amount of data points obtained continuously during the bending test of each nanofibre. We want to emphasize that this is one of the main values of this work, as this self-consistency check has not been previously reported in the literature.[35–37] Fig. 5 shows a force-volume map and the extraction of the mechanical parameters from it. The slope from the contact regime was evaluated at mid-way of the hanging profile for a given nanofibre but imaged with two different cantilevers (with different spring constants).

The slope values obtained from this two-fold characterization yielded 2.53 and 4.24 nN nm^{-1}, respectively. When such values are introduced into eqn (1), it results that the elastic modulus of the sepiolite fibre measured with two different AFM probes in force volume mode is 4.7 and 6.6 GPa, respectively. These values are a strong confirmation of the results obtained using the sequential topographic imaging strategy, which were 4.8 and 6.0 GPa, respectively. It should be noted that in FV measurements the error involved in the determination of the middle point of the fibre is higher as the spatial data sampling is smaller than in standard topographical imaging. This agreement confirms the consistency (and complementarity) between both techniques.

In a complementary way to the elastic properties determined at the single fibre level, nanoindentation and macroscopic compression measurements on sepiolite blocks (as recovered

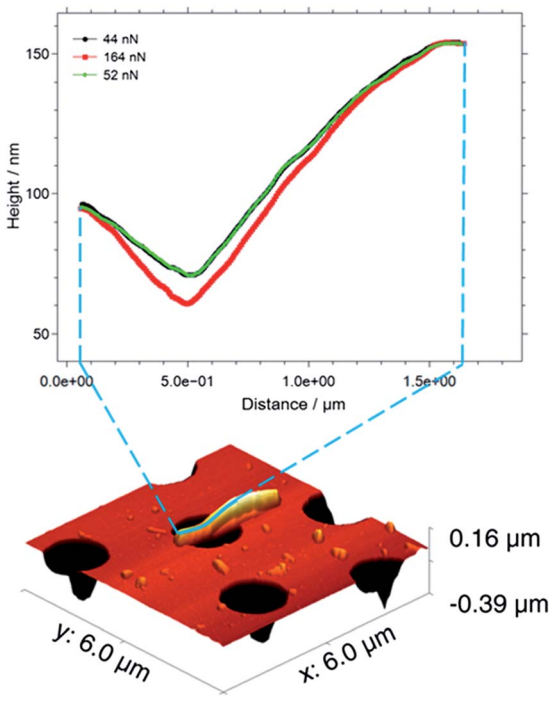

Fig. 4 On top, deflection profiles of sample S2.Hk (see ESI† for details about the samples and notation) at the lowest force applied (44 nN) and at the highest applied force (164 nN) followed by the low force deflection profile (52 nN) measured after the entire bending experiment. The spatial stability of the nanofibre as well as the reversibility of the deformation are evidenced.

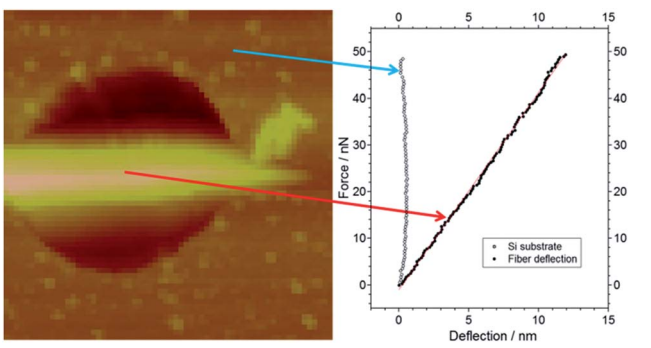

Fig. 5 Topographic image of sample S3.Hk (see ESI† for details about the samples and notation) as imaged by force volume (top picture) and force curves from two different points of the sample. The top point, corresponding to the silicon substrate, shows a force profile typical of an infinitely hard surface with a quasi-vertical slope in the contact regime. On the other hand, the middle point, located half-way of the hanging sepiolite fibre, shows an interaction profile that directly reflects the relation between the applied force and the fibre deflection.

from the clay deposits) were also performed. Nanoindentation was selected as a characterization technique halfway between the nano- and the macroscale. This technique implies, thus, a variation over the previously studied length scale (the single sepiolite fibre cross section) of more than four orders of magnitude. From the indentation essay, the so-called reduced elastic modulus could be determined between 1 and 5.5 GPa, with an average value of 2.93 GPa. To further assay the effect of sepiolite organization on the mechanical properties macroscopic, blocks were also tested by conventional mechanical compression. On average, the compressive modulus was determined to be of 398 MPa (sd = 38 MPa).

Discussion

The first element to discuss regarding the mechanical characterization of sepiolite is its variability across the different length scales tested. In fact, from nanoscale using the AFM, to macroscale using the universal testing machine, sepiolite presents considerably different elastic moduli. Fig. 6 displays the elastic properties of sepiolite at different length scales in a log–log plot. As depicted, not only the elastic modulus varies along the length scales but also these two parameters are related trough a linear trend in the log–log plot.

Although AFM and nanoindentation do deal with the most basic mechanical properties of sepiolite, in which aggregation effects do not play an important role, we find remarkable the scaling behaviour of the elastic modulus among several orders of magnitude. Since a single sepiolite fibre corresponds to a single sepiolite crystal, the AFM measurements (which were measured over single fibres) correspond to the highest order of sepiolite. It is therefore expected that its mechanical properties are maximized. On the other hand when analysing sepiolite blocks (by macroscopic compression tests) the material is at its highest disorder level, because it is composed of randomly oriented sepiolite fibres aggregated into a monolith. Such disorder is consistent with the low value determined for the monolith's elastic modulus. In the sepiolite case, the density relation with the elastic modulus also seems to apply. Calculating the theoretical density for sepiolite based on its half-unit cell formula ($Si_{12}O_{30}Mg_8(OH)_4(H_2O)_4 \cdot 8H_2O$) and its unit cell volume of 1880 Å^3 results in a theoretical density value around 2.2 g cm^{-3}. On the other hand, an etymological look at sepiolite's synonym "Meerschaum" yields sea foam, such name was given after the whitish blocks of sepiolite found floating in the sea. That information indicates that the density of sepiolite blocks is inferior to that of sea water. Also, laboratory measurements performed on sepiolite blocks with a clearly defined geometry rendered density values around 0.7 g cm^{-3}. As in other natural nanomaterials such as wood or bone, sepiolite's elastic properties span over several orders of magnitude according to their organizational level[1] which is, in turn, closely related to the material's density. However, the degradation of the mechanical properties of sepiolite from the single crystalline fibre to the more disorganized level seems to scale according to a stiffness guideline proportional to $E^{1/3}/\rho$. Other composite materials based on nanoparticles of biological origin such as bone and wood often scale according to $E^{1/2}/\rho$.[38] The difference in the power law scaling between these eminently porous materials has already been brought up in the beginning of the manuscript. While nanocomposites of biological origin are highly organized materials and display optimized mechanical properties at different length scales, nanoparticles of geological origin such as clay minerals are usually arranged in an isotropic manner rendering the macroscopic materials significantly less efficient. Disassembling less organized geological systems seems thus more efficient as a natural nanoparticle preparation strategy than the similar procedure in biological derived systems.

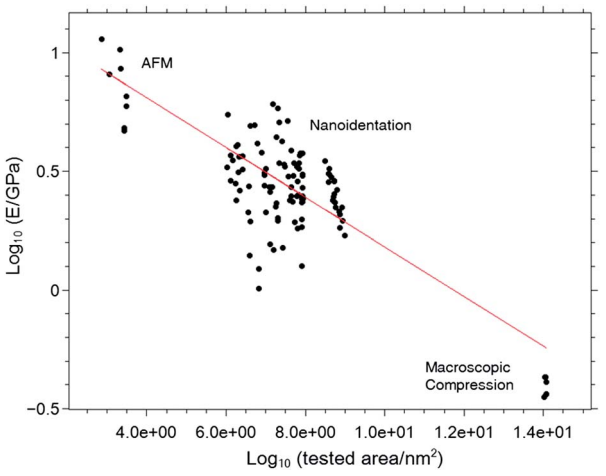

Fig. 6 Graphical representation in logarithmic scale of the elastic properties of sepiolite according to the length scale/technique employed. The length scales are defined as: the fibre average cross-section for AFM measurements; the irreversibly indented area (24.5 × Pd^2, where Pd stands for plastic depth) for nanoindentation experiments, and the monolith cross-section for macroscopic compression experiments.

Conclusions

In summary, the present work discloses the first individual direct measurement of the elastic properties of single sepiolite crystals. Moreover, it makes use of different experimental approaches under the AFM to assess the bending modulus of sepiolite which has been previously grafted onto a micro-patterned silicon substrate. The obtained elastic modulus of 8.2 GPa will allow, from now onwards, to rationally design nanocomposites reinforced with sepiolite nanofibres. Additionally, the elastic properties of sepiolite have been compared across length scales, from the macroscopic block as obtained from the pit to the nanofibre level and the scaling between the material density and elastic properties disclosed. Finally, and as a consequence of such multiscale measurements, the rationale behind the disassembling of bio- and geo-nanoparticle systems has been discussed.

Acknowledgements

This work has been supported by Ministerio de Economía y Competitividad (CICYT, Spain, MAT2009-09960, MAT2012-

31759, FIS2009-12964-C05-03 and FIS2012-38866-C05-05) and Comunidad Autónoma de Madrid (Project N8. S2009/PPQ-1642, AVANSENS). We thank J. Ortiz (CSIC) for performing the nanoindentation experiments and A. Valera (CSIC) for FE-SEM images.

Notes and references

1 P. Fratzl and R. Weinkamer, *Prog. Mater. Sci.*, 2007, **52**, 1263–1334.
2 X. D. Li, W. C. Chang, Y. J. Chao, R. Z. Wang and M. Chang, *Nano Lett.*, 2004, **4**, 613–617.
3 A. Usuki, Y. Kojima, M. Kawasumi, A. Okada, Y. Fukushima, T. Kurauchi and O. Kamigaito, *J. Mater. Res.*, 1993, **8**, 1179–1184.
4 Y. Kojima, A. Usuki, M. Kawasumi, A. Okada, Y. Fukushima, T. Kurauchi and O. Kamigaito, *J. Mater. Res.*, 1993, **8**, 1185–1189.
5 K. Brunauer and A. Preisinger, *Tschermaks Mineral. Petrogr. Mitt.*, 1956, **6**, 120–140.
6 E. Ruiz-Hitzky, M. Darder, P. Aranda, M. A. M. del Burgo and G. del Real, *Adv. Mater.*, 2009, **21**, 4167–4171.
7 A. Gomez-Aviles, M. Darder, P. Aranda and E. Ruiz-Hitzky, *Angew. Chem., Int. Ed.*, 2007, **46**, 923–925.
8 A. Gómez-Avilés, M. Darder, P. Aranda and E. Ruiz-Hitzky, *Appl. Clay Sci.*, 2010, **47**, 203–211.
9 E. Ruiz-Hitzky, M. Darder, F. M. Fernandes, E. Zatile, F. J. Palomares and P. Aranda, *Adv. Mater.*, 2011, **23**, 5250–5255.
10 M. Darder, M. Lopez-Blanco, P. Aranda, A. J. Aznar, J. Bravo and E. Ruiz-Hitzky, *Chem. Mater.*, 2006, **18**, 1602–1610.
11 M. Darder, P. Aranda and E. Ruiz-Hitzky, *Adv. Mater.*, 2007, **19**, 1309–1319.
12 F. Chivrac, E. Pollet and L. Avérous, *Mater. Sci. Eng., R*, 2009, **67**, 1–17.
13 N. Olmo, M. A. Lizarbe and J. G. Gavilanes, *Biomaterials*, 1987, **8**, 67–69.
14 F. M. Fernandes, A. I. Ruiz, M. Darder, P. Aranda and E. Ruiz-Hitzky, *J. Nanosci. Nanotechnol.*, 2009, **9**, 221–229.
15 F. M. Fernandes, I. Manjubala and E. Ruiz-Hitzky, *Phys. Chem. Chem. Phys.*, 2011, **13**, 4901–4910.
16 F. M. Fernandes, M. Darder, A. I. Ruiz, P. Aranda and E. Ruiz-Hitzky, in *Nanocomposites with Biodegradable Polymers. Synthesis, Properties, and Future Perspectives*, ed. V. Mittal, Oxford University Press, New York, 2011.
17 A. Nohales, L. Solar, I. Porcar, C. I. Vallo and C. M. Gomez, *Eur. Polym. J.*, 2006, **42**, 3093–3101.
18 J. L. Ahlrichs, C. Serna and J. M. Serratosa, *Clays Clay Miner.*, 1975, **23**, 119–124.
19 C. Serna, J. L. Ahlrichs and J. M. Serratosa, *Clays Clay Miner.*, 1975, **23**, 452–457.
20 P. F. Barron and R. L. Frost, *Am. Mineral.*, 1985, **70**, 758–766.
21 E. Ruiz-Hitzky, *J. Mater. Chem.*, 2001, **11**, 86–91.
22 R. T. Cygan, J.-J. Liang and A. G. Kalinichev, *J. Phys. Chem. B*, 2004, **108**, 1255–1266.
23 M. A. Mazo, L. I. Manevitch, E. B. Gusarova, A. A. Berlin, N. K. Balabaev and G. C. Rutledge, *J. Phys. Chem. C*, 2008, **112**, 17056–17062.
24 D. A. Kunz, E. Max, R. Weinkamer, T. Lunkenbein, J. Breu and A. Fery, *Small*, 2009, **5**, 1816–1820.
25 J. W. Suk, R. D. Piner, J. An and R. S. Ruoff, *Thin Solid Films*, 2013, **527**, 205–209.
26 M. A. Hopcroft, W. D. Nix and T. W. Kenny, *J. Microelectromech. Syst.*, 2010, **19**, 229–238.
27 R. S. Faibish, W. Yoshida and Y. Cohen, *J. Colloid Interface Sci.*, 2002, **256**, 341–350.
28 H.-J. Butt, B. Cappella and M. Kappl, *Surf. Sci. Rep.*, 2005, **59**, 1–152.
29 S. Iwamoto, W. Kai, A. Isogai and T. Iwata, *Biomacromolecules*, 2009, **10**, 2571–2576.
30 W. C. Oliver and G. M. Pharr, *J. Mater. Res.*, 2004, **19**, 3–20.
31 H. Gercek, *Int. J. Rock Mech. Min. Sci.*, 2007, **44**, 1–13.
32 J.-P. Salvetat, J.-M. Bonard, N. H. Thomson, A. J. Kulik, L. Forró, W. Benoit and L. Zuppiroli, *Appl. Phys. A: Mater. Sci. Process.*, 1999, **69**, 255–260.
33 J.-P. Salvetat, G. Briggs, J.-M. Bonard, R. Bacsa, A. Kulik, T. Stöckli, N. Burnham and L. Forró, *Phys. Rev. Lett.*, 1999, **82**, 944–947.
34 J. M. Gere, *Mechanics of Materials*, Brooks/Cole, Pacific Grove, CA, 5th edn, 2001.
35 J. Salvetat-Delmotte, *Carbon*, 2002, **40**, 1729–1734.
36 W. R. Bowen, R. W. Lovitt and C. J. Wright, *Biotechnol. Lett.*, 2000, **22**, 893–903.
37 M. M. J. F. Koenders, L. Yang, R. G. Wismans, K. O. van der Werf, D. P. Reinhardt, W. Daamen, M. L. Bennink, P. J. Dijkstra, T. H. van Kuppevelt and J. Feijen, *Biomaterials*, 2009, **30**, 2425–2432.
38 M. F. Ashby, L. J. Gibson, U. Wegst and R. Olive, *Proc. R. Soc. A*, 1995, **450**, 123–140.